

## Diffusion of zinc vacancies and interstitials in zinc oxide

Paul Erhart<sup>a)</sup> and Karsten Albe

Institut für Materialwissenschaft, Technische Universität Darmstadt, Petersenstraße 23,  
D-64287 Darmstadt, Germany

(Received 6 March 2006; accepted 26 April 2006; published online 18 May 2006)

The self-diffusion coefficient of zinc in ZnO is derived as a function of the chemical potential and Fermi level from first-principles calculations. Density functional calculations in combination with the climbing image-nudged elastic band method are used in order to determine migration barriers for vacancy, interstitial, and interstitialcy jumps. Zinc interstitials preferentially diffuse to second nearest neighbor positions. They become mobile at temperatures as low as 90–130 K and therefore allow for rapid defect annealing. Under predominantly oxygen-rich and *n*-type conditions self-diffusion occurs via a vacancy mechanism. © 2006 American Institute of Physics.

[DOI: 10.1063/1.2206559]

Zinc oxide is currently under intensive investigation because of its various applications in electronic and optoelectronic devices, where point defect engineering is of crucial importance. Therefore, understanding the thermodynamics and kinetics of intrinsic point defects in ZnO is not only of fundamental but also significant technological interest. Zinc migration has been discussed, in particular, with respect to the degradation of varistor devices<sup>1,2</sup> which is believed to proceed through the migration of intrinsic defects, most likely zinc interstitials, in the vicinity of grain boundaries. Knowledge of individual defect diffusivities is also instrumental in order to control the formation of unwanted and compensating defects, which are likely to contribute to the difficulties in synthesizing *p*-type zinc oxide (see, e.g., Refs. 3 and 4). A large number of studies have been conducted to measure the self-diffusion of zinc in ZnO.<sup>5–15</sup> The experimental data, however, exhibit a considerable spread which renders their interpretation difficult. In view of this situation, a theoretical approach can provide valuable insights into the various atomistic migration processes and help to quantify their respective contributions.

In this letter we present an analysis of the migration paths and the diffusivities of zinc in ZnO. Migration energies are determined by total energy calculations within density functional theory (DFT) using the Vienna *ab initio* simulation package<sup>16</sup> (VASP) with the projector-augmented wave (PAW) method.<sup>17,18</sup> The GGA+*U* scheme with  $\bar{U}-\bar{J}=7.5$  eV in the formulation by Dudarev *et al.*<sup>19</sup> was adopted to properly describe the band structure of zinc oxide.<sup>20</sup> Hexagonal 32-atom supercells equivalent to  $2 \times 2 \times 2$  primitive unit cells were employed. The plane-wave energy cutoff was set to 500 eV and a  $\Gamma$  point centered  $2 \times 2 \times 2$  *k*-point grid was used for Brillouin zone sampling. In order to determine migration paths and barriers, the climbing image-nudged elastic band (CI-NEB) method was employed.<sup>21,22</sup> We considered first and second nearest neighbor paths and all relevant charge states for vacancy as well as interstitial migration. Migration paths involving antisite defects were not considered because of high antisite formation enthalpies.<sup>23–25</sup> Further computational details can be found in Ref. 26. The

error of the calculated migration energies is estimated to be on the order of 0.1 eV or less.<sup>26</sup>

The wurtzite structure is composed of two interpenetrating hexagonal close packed sublattices, which are occupied by oxygen and zinc atoms, respectively. If we consider vacancy jumps to first or second nearest neighbor positions on the zinc sublattice, three mechanisms can be distinguished [see Fig. 1(a)]: in-plane migration to first nearest neighbors (process A), out-of-plane migration to first nearest neighbors (process B), and out-of-plane migration to second nearest neighbors (process C).

The corresponding migration barriers are compiled in Table I. For vacancies migration by out-of-plane jumps to first nearest neighbors (path B) is energetically preferred. The barrier for this path decreases from 1.19 to 0.77 eV going from the neutral to the doubly negative charge state. Taking into account the projections of the displacement vector perpendicular and parallel to the  $\langle 0001 \rangle$  direction, path B leads to nearly isotropic diffusion.

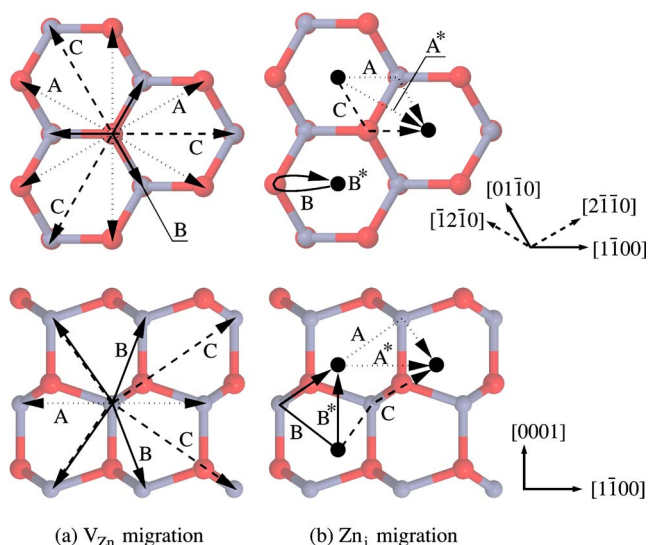


FIG. 1. (Color online) Diffusion paths accessible to (a) zinc vacancies and (b) zinc interstitials on the wurtzite lattice via jumps to first or second nearest neighbor sites. A—in-plane migration to first nearest neighbors, B and C—out-of-plane migration to first and second nearest neighbors, respectively. Interstitial mechanisms (in contrast to interstitialcy mechanisms) are marked with asterisks.

<sup>a)</sup>Electronic mail: paul.erhart@web.de

TABLE I. Energy barriers for vacancy and interstitial mediated migration of zinc in units of eV.

Migration path	Charge state			
	$q=0$	$q=-1$	$q=-2$	
Zinc vacancy $V_{Zn}$				
First nearest neighbor: in plane	A	1.36	1.33	1.51
First nearest neighbor: out of plane	B	1.19	1.12	0.77
Second nearest neighbor: out of plane	C	2.86	2.81	2.56
Formation enthalpy		5.60	5.96	7.06
Zinc interstitial $Zn_i$				
First nearest neighbor: in plane	A*	0.33	0.40	0.25
First nearest neighbor: in plane	A	0.89	0.69	0.90
First nearest neighbor: out of plane	B*	1.44	1.34	1.28
First nearest neighbor: out of plane	B	0.33	0.40	0.47
First nearest neighbor: out of plane	C	0.22	0.27	0.52
Formation enthalpy		0.02	1.69	4.25

Zinc interstitials occupy the octahedral interstitial sites of the wurtzite lattice located at the centers of the hexagonal  $\langle 0001 \rangle$  channels. The interstitial sites span a simple hexagonal lattice with an axial ratio which is half as large as the one of the underlying wurtzite lattice. The resulting migration paths are shown in Fig. 1(b). Ion migration can occur both via pure *interstitial mechanisms*, i.e., via jumps on the simple hexagonal interstitial site lattice, and via *interstitialcy mechanisms*. In the latter case the interstitial atom pushes out one of its zinc neighbors which then becomes an interstitial atom itself. In-plane migration of zinc interstitials can occur via jumps to first nearest neighbor zinc interstitial sites along  $\langle 2\bar{1}10 \rangle$  (process A\*). Equivalently, out-of-plane motion is possible by first-neighbor jumps through the  $\langle 0001 \rangle$  channels of the wurtzite lattice (process B\*). In-plane and out-of-plane motions can also occur via interstitialcy mechanisms involving first nearest neighbors; the interstitialcy mechanisms A and B shown in Fig. 1(b) and the interstitial mechanisms A\* and B\* lead to equivalent final configurations. Finally, out-of-plane motion via second-nearest neighbor sites is also possible via interstitialcy mechanism C equivalent to an effective displacement of  $a/\sqrt{6}\langle 2\bar{1}10 \rangle + c/2\langle 0001 \rangle$ .

For any charge state the smallest (dominant) migration barrier is just about a few tenths of an eV (Table I) which implies that zinc interstitials should be mobile down to very low temperatures. If we assume a typical annealing time of 10 min and a mean square displacement of  $10^4 - 10^6 \text{ nm}^2$ , the onset of defect mobility can be estimated using the Einstein relation. With an exponential prefactor of 8 THz one obtains threshold temperatures for zinc interstitial migration between 90 and 110 K ( $q=+2$ ), 110 and 130 K ( $q=+1$ ), and 100 and 120 K ( $q=0$ ). This is in excellent agreement with annealing experiments which find mobile intrinsic defects at temperatures as low as 80–130 K.<sup>27–29</sup>

Notably, with the only exception of the neutral charge state, the lowest migration barriers are obtained for the second neighbor mechanism (process C). Similar to the case of path B for vacancy diffusion, process C involves both in-plane and out-of-plane displacements and leads to quasi-isotropic diffusion characteristics. In contrast, interstitial migration along the  $\langle 0001 \rangle$  channels of the wurtzite lattice (process B) is energetically rather unfavorable. Our analysis of the site-projected electronic density of states for the migrating zinc atoms shows the saddle point configuration

along path C to deviate the least from the ideal configuration, leading to a very small energy difference between the initial and the transition state.

Migration barriers for zinc vacancies and interstitials have been previously calculated by Binks and Grimes using analytical pair potentials in combination with a shell-model description of the oxygen ions (see Refs. 30 and 12, and references therein). They considered jumps to first nearest neighbors only and did not include interstitialcy mechanisms. In the past, these results were frequently used to interpret experiments and, in particular, to discriminate between interstitial and vacancy mechanisms (see Ref. 12 and references therein). With respect to the doubly negative zinc vacancy ( $V_{Zn}''$ ) we find at least reasonable agreement between the shell-model potential calculations and our DFT data. According to Ref. 12 the barriers for processes A and B are 1.81 and 0.91 eV, respectively, while the present calculations give values of 1.51 and 0.77 eV. For the zinc interstitial, there are, however, significant differences: the DFT barriers are in general smaller and in contrast to the analytical potential calculations indicate nearly isotropic diffusion.

The detailed knowledge of all relevant migration paths and related barriers allows us to calculate the self-diffusion coefficient.<sup>26</sup> Thereby, a more detailed assessment of the experimental data becomes possible. In the case of an intrinsic

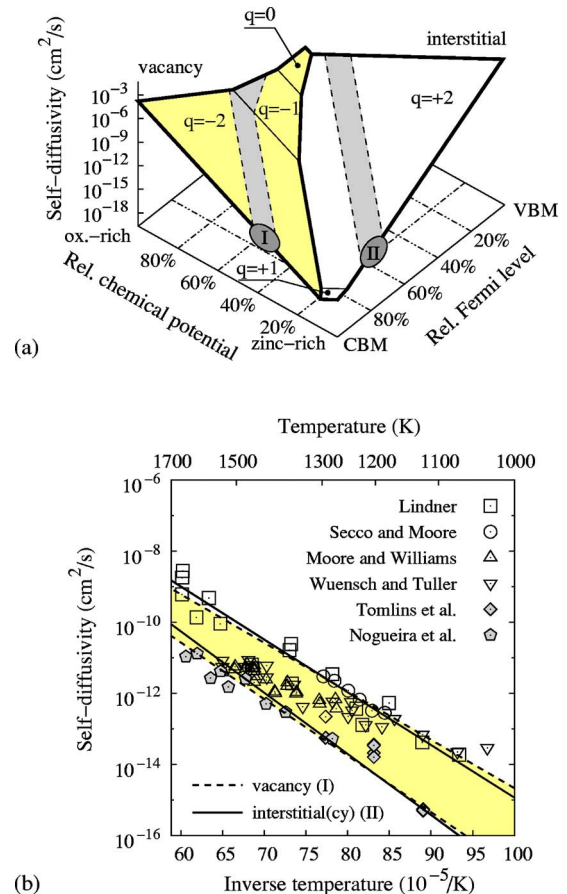


FIG. 2. (Color online) (a) Dependence of self-diffusion coefficient on Fermi level and chemical potential and (b) temperature dependence of calculated self-diffusion coefficient in comparison with experimental data: Lindner (1952, MTS, Ref. 5), Secco and Moore (1955/1957, GE, Refs. 9 and 10), Moore and Williams (1959, MTS, Ref. 11), Wuensch and Tuller (1994, MTS, Ref. 15), Tomlins *et al.* (2000, SIMS, Ref. 12), and Nogueira *et al.* (2003, MTS, Ref. 13). MTS—method of thin sections, GE—gaseous exchange, and SIMS—secondary ion mass spectroscopy.

mechanism the activation energy for self-diffusion comprises not only the defect migration barriers but also the formation enthalpies of the defects involved.<sup>26,31</sup> Since the defect formation enthalpies vary linearly with the chemical potential and Fermi level,<sup>32</sup> the self-diffusion constant will strongly depend on these parameters. The variation of the self-diffusion coefficient with the chemical potential and Fermi level as derived from our calculations is shown for a temperature of 1300 K in Fig. 2(a) where the defect formation enthalpies from Ref. 20 were used. The light gray shaded stripes bracketed by dashed lines indicate the experimental data range at this temperature. Since Fermi level and chemical potential are unknown for these experiments a more direct comparison is not possible. For two exemplifying combinations of Fermi level and chemical potential [dark gray shaded areas I and II in Fig. 2(a)] the temperature dependence of the diffusivity is shown in Fig. 2(b). Both mechanisms reproduce the experimentally observed dependence. The analysis illustrates that vacancy mediated diffusion can explain the experimental data for Fermi levels close to the conduction band minimum (CBM) and chemical potentials which tend to oxygen-rich conditions. In the opposite case zinc interstitial mediated diffusion should dominate. Since most often ZnO is *n*-type conducting the diffusion studies in the literature most likely sampled zinc vacancy mediated self-diffusion.

Together with the results presented in Ref. 26 it is now possible to establish a hierarchy for the mobilities of intrinsic defects in zinc oxide. The most mobile defects are zinc interstitials followed by oxygen interstitials, zinc vacancies, and oxygen vacancies. These data provide further support for the most widely discussed model for degradation of zinc oxide based varistors. This model assumes zinc interstitials to migrate in the vicinity of grain boundaries and oxygen vacancies to be rather immobile (see, e.g., Refs. 1 and 2). It is also noteworthy that zinc oxide shows a remarkable radiation hardness.<sup>28</sup> The high mobilities of intrinsic interstitial defects are likely to contribute to this behavior, since they allow for rapid annealing of Frenkel pairs or defect agglomerates.

In the present letter, we studied the migration of zinc interstitials and vacancies in zinc oxide by means of density functional theory calculations. Where comparison with experiment is possible we find generally good agreement. Zinc interstitials are the most mobile defect contributing to annealing at temperatures as low as 90–130 K. The calculations further indicate that for *n*-type conducting ZnO intrinsic self-diffusion occurs via a vacancy mechanism. We anticipate the results of this study to be very useful for the (re-)interpretation of diffusion experiments. Furthermore, in

conjunction with data for the migration of oxygen<sup>26</sup> and defect formation enthalpies<sup>20</sup> they allow us to develop consistent models for device simulations.

The authors would like to thank H. Jónsson, G. Henkelman, and their co-workers for kindly providing their VASP extensions and acknowledge generous grants of computer time at the Hessischer Hochleistungsrechner through the Hochschulrechenzentrum at the Technische Universität Darmstadt. This project was funded by the Sonderforschungsbereich 595 “Fatigue in functional materials” of the Deutsche Forschungsgemeinschaft.

- <sup>1</sup>T. K. Gupta and W. Carlson, *J. Mater. Sci.* **20**, 3487 (1985).
- <sup>2</sup>M. Ramanachalam, A. Rohatgi, J. Schaffer, and T. K. Gupta, *J. Appl. Phys.* **69**, 8380 (1991).
- <sup>3</sup>D. C. Look, B. Claffin, Y. I. Alivov, and S. J. Park, *Phys. Status Solidi A* **201**, 2203 (2004).
- <sup>4</sup>D. C. Look and B. Claffin, *Mater. Res. Soc. Symp. Proc.* **829**, B8.6.1 (2005).
- <sup>5</sup>R. Lindner, *Acta Chem. Scand.* (1947-1973) **6**, 457 (1952).
- <sup>6</sup>J. P. Roberts and C. Wheeler, *Philos. Mag.* **2**, 708 (1957).
- <sup>7</sup>J. P. Roberts and C. Wheeler, *Trans. Faraday Soc.* **56**, 570 (1960).
- <sup>8</sup>D. G. Thomas, *J. Phys. Chem. Solids* **3**, 229 (1957).
- <sup>9</sup>E. A. Secco and W. J. Moore, *J. Chem. Phys.* **23**, 1170 (1955).
- <sup>10</sup>E. A. Secco and W. J. Moore, *J. Chem. Phys.* **26**, 942 (1957).
- <sup>11</sup>W. J. Moore and E. L. Williams, *Discuss. Faraday Soc.* **28**, 86 (1959).
- <sup>12</sup>G. W. Tomlins, J. L. Routbort, and T. O. Mason, *J. Appl. Phys.* **87**, 117 (2000).
- <sup>13</sup>M. A. d. N. Nogueira, W. B. Ferraz, and A. C. S. Sabioni, *Mater. Res.* **6**, 167 (2003).
- <sup>14</sup>M. Nogueira, A. Sabioni, and W. Ferraz, *Defect Diffus. Forum* **237–240**, 163 (2005).
- <sup>15</sup>B. J. Wuensch and H. L. Tuller, *J. Phys. Chem. Solids* **55**, 975 (1994).
- <sup>16</sup>G. Kresse and J. Furthmüller, *Phys. Rev. B* **54**, 11169 (1996).
- <sup>17</sup>P. E. Blöchl, *Phys. Rev. B* **50**, 17953 (1994).
- <sup>18</sup>G. Kresse and D. Joubert, *Phys. Rev. B* **59**, 1758 (1999).
- <sup>19</sup>S. L. Dudarev, G. A. Botton, S. Y. Savrasov, C. J. Humphreys, and A. P. Sutton, *Phys. Rev. B* **57**, 1505 (1998).
- <sup>20</sup>P. Erhart, K. Albe, and A. Klein, *Phys. Rev. B* **73**, 205203 (2006).
- <sup>21</sup>G. Henkelman, G. Jóhannesson, and H. Jónsson, *Progress on Theoretical Chemistry and Physics* (Kluwer Academic, Dordrecht, 2000), p. 269.
- <sup>22</sup>G. Henkelman, B. P. Uberuaga, and H. Jónsson, *J. Chem. Phys.* **113**, 9901 (2000).
- <sup>23</sup>A. F. Kohan, G. Ceder, D. Morgan, and C. G. Van de Walle, *Phys. Rev. B* **61**, 15019 (2000).
- <sup>24</sup>S. B. Zhang, S. H. Wei, and A. Zunger, *Phys. Rev. B* **63**, 075205 (2001).
- <sup>25</sup>F. Oba, S. R. Nishitani, S. Isotani, H. Adachi, and I. Tanaka, *J. Appl. Phys.* **90**, 824 (2001).
- <sup>26</sup>P. Erhart and K. Albe, *Phys. Rev. B* **73**, 115207 (2006).
- <sup>27</sup>Y. V. Gorelinskii and G. D. Watkins, *Phys. Rev. B* **69**, 115212 (2004).
- <sup>28</sup>C. Coskun, D. C. Look, G. C. Farlow, and J. R. Sizelove, *Semicond. Sci. Technol.* **19**, 752 (2004).
- <sup>29</sup>K. Lorenz, E. Alves, E. Wendler, O. Bilani, W. Wesch, and M. Hayes, *Appl. Phys. Lett.* **87**, 191904 (2005).
- <sup>30</sup>D. J. Binks and R. W. Grimes, *J. Am. Ceram. Soc.* **76**, 2370 (1993).
- <sup>31</sup>A. R. Allnatt and A. B. Lidiard, *Atomic Transport in Solids* (Cambridge University Press, Cambridge, 2003).
- <sup>32</sup>S. B. Zhang and J. E. Northrup, *Phys. Rev. Lett.* **67**, 2339 (1991).